# Inline $\mathrm{TM}_{110}$-Mode Filters With High-Design Flexibility by Utilizing Bypass Couplings of Nonresonating $\mathrm{TE}_{10/01}$ Modes

Uwe Rosenberg, *Senior Member, IEEE*, Smain Amari, *Member, IEEE*, and Jens Bornemann, *Fellow, IEEE*

***Abstract*—This paper presents a new class of pseudoelliptic function filters that are based on compact inline $\mathrm{TM}_{110}$-mode cavity configurations. No structural folding is required. The bypass couplings are implemented through the nonresonating $\mathrm{TE}_{10/01}$ modes so that arbitrarily positioned transmission zeros can be implemented. Design guidelines to generate a given transmission zero on the desired side of the passband and how to control it are presented. To demonstrate its flexibility, the approach is illustrated at examples of four-pole inline filters providing Chebyshev, elliptic-function-type, and asymmetric characteristics. Performance comparisons with different numerical codes validate the designs. A fourth-order pseudoelliptic filter with four transmission zeros is then designed, constructed, and measured. Excellent agreement between simulated and experimental results verifies the approach.**

***Index Terms*—Bandpass filters, elliptic function filters, filter synthesis, waveguide filters.**

## I. INTRODUCTION

ELLIPTIC and pseudoelliptic function filters are finding widespread application in modern communication systems where sharp cutoff skirts are required for efficient use of an already crowded and limited electromagnetic spectrum. These classes of filters exhibit transmission zeros at finite frequencies in the complex plane and are often implemented by introducing structural folding to allow cross-coupling, or by using dual and multimode resonators in inline topologies [1]–[4]. The extracted pole technique also allows the implementation of pseudoelliptic transfer functions [5]. Transmission zeros at real frequencies can also be implemented by using strongly dispersive coupling [6].

In the actual design of pseudoelliptic cross-coupled resonator filters, the bypass or cross-couplings are most often represented by coupling slots, irises, coupling screws, or other physical elements. Another mechanism that has been reported in the literature is the use of higher order modes to provide additional paths for the signal between different points in inline structures [7], [8]. A limitation of such an approach is the fact that the resulting transmission zeros are positioned in the upper stopband of the filter. Furthermore, it is not easy, and even impossible, to position these zeros arbitrarily close to the passband [8].

Manuscript received October 8, 2002; revised January 29, 2003.

U. Rosenberg is with Marconi Communications GmbH, D-71522 Backnang, Germany (e-mail: Uwe.Rosenberg@marconi.com).

S. Amari is with the Department of Electrical and Computer Engineering, Royal Military College of Canada, Kingston, ON, Canada K7K 7B4 (e-mail: Smain.Amari@rmc.ca).

J. Bornemann is with the Department of Electrical and Computer Engineering, University of Victoria, Victoria, BC, Canada V8W 3P6 (e-mail: jbornema@ece.uvic.ca).

Digital Object Identifier 10.1109/TMTT.2003.812577

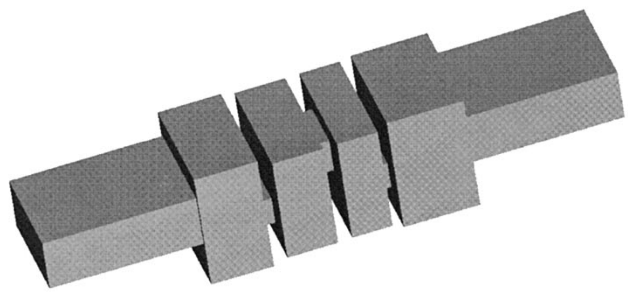

Fig. 1. Novel $\mathrm{TM}_{110}$-mode inline filter structure utilizing bypass couplings of nonresonating $\mathrm{TE}_{10/01}$ modes.

An examination of the inline structures implementing transmission zeros at finite frequencies shows that they are based on $\mathrm{TE}_{101}$ resonances in rectangular waveguide [7], [8]. However, with this choice of resonances, the inline configuration allows only coupling of the magnetic field components. The size and location of irises is used to control the desired coupling between the adjacent resonators. Asymmetric iris locations provide only exiguous bypass couplings by nonresonating cavity modes, thereby severely limiting the range of transfer functions that can be realized [7]–[9]. In order to extend the design capability of inline structures in rectangular waveguide, it is, therefore, imperative to have more degrees of freedom in regard to the nature of the coupling allowed by the chosen resonances and the mechanism used to implement bypass couplings. A simple alternative, which allows both magnetic, electric, and mixed coupling between resonators in inline structures in the rectangular waveguide, is to use $\mathrm{TM}_{110}$ resonances. An examination of the field distribution of this type of resonance shows that by properly positioning the coupling slot (iris) between two adjacent cavities, it is possible to control the strength and nature (sign) of the coupling.

In this paper, we propose a new class of compact inline $\mathrm{TM}_{110}$-mode filters that implement elliptic and pseudoelliptic function responses (Fig. 1).

In these filters, the transmission zeros are generated by exploiting nonresonating modes in the structure to provide additional paths for the power flow between adjacent resonators. By properly adjusting the coupling to these modes and their relative phases, it will be shown that pseudoelliptic responses, with arbitrarily positioned transmission zeros, can be implemented

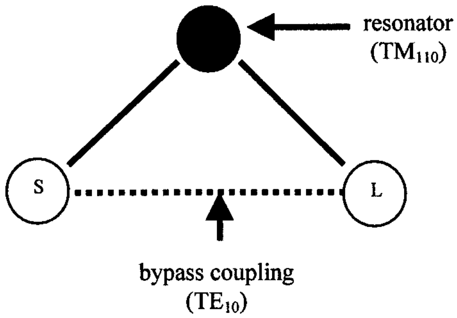


Fig. 2. Coupling and routing scheme from source (S) to load (L) for a singlet (one resonator, one transmission zero).

using rather simple geometries in rectangular waveguide technology. All couplings are basically realized by magnetic-field components of the respective modes of the cavities and interface waveguides, However, their nature may be inductive or capacitive depending on the dimensions of the coupling iris. Therefore, for a special filter design, inductive, capacitive, or both coupling types can be used, thus providing additional flexibility to tailor the far-out-of-band rejection of the introduced filter type (see Section III).

To the best of our knowledge, inline $\mathrm{TM}_{110}$-mode cavity filters providing elliptic and pseudoelliptic function responses have not been reported before.

## II. Guidelines for Initial Design

### A. Operational Principle of a Singlet

The presence of a visible passband in the initial design can be achieved by determining the dimensions of the resonators such that their resonant frequency is equal or close to the center of the passband. In the case of a rectangular cavity of width $a$, height $b$, and length $c$, the resonant frequency of $\mathrm{TM}_{110}$ resonances is known analytically and is given by

$$f_r = \frac{v_c}{2}\sqrt{\frac{1}{a^2} + \frac{1}{b^2}} \tag{1}$$

where $v_c$ is the speed of light in vacuum. Note that the resonant frequency does not depend on the length of the cavity (in the $z$-direction). On the other hand, the resonant frequency of the $\mathrm{TE}_{101}$ is given by

$$f_r = \frac{v_c}{2}\sqrt{\frac{1}{a^2} + \frac{1}{c^2}}. \tag{2}$$

From (1) and (2), it is obvious that the dimensions of the cavity can be chosen such that $\mathrm{TM}_{110}$ is resonating while $\mathrm{TE}_{101}$ is not and can be used to implement the bypass couplings.

The next step is to position the transmission zeros as close as possible to their desired location. This is achieved by carefully examining the field distributions at the eventual position of the coupling slot in order to determine the strength of the coupling coefficients and their relative signs. Consider, for example, the implementation of a transmission zero on the upper side of the passband using a rectangular cavity resonating in the $\mathrm{TM}_{110}$ mode and the nonresonating $\mathrm{TE}_{101}$ mode as a bypass mechanism. The coupling and routing scheme of this one-resonator–one-transmission-zero structure is shown in Fig. 2 and is referred to as a singlet, in analogy with triplets and quadruplets, since only one resonator is used to generate a filtering response with one transmission zero.

An examination of the corresponding synthesis problem shows that the coupling coefficients are all positive for a transmission zero in the upper stopband [10]. For example, if a zero is located at normalized frequency $\Omega = 6$ and the in-band return loss is 20 dB, the coupling matrix corresponding to Fig. 2 is

$$M = \begin{bmatrix} 0.0000 & 1.3043 & 0.5647 \\ 1.3043 & -2.9877 & 1.3043 \\ 0.5647 & 1.3043 & 0.0000 \end{bmatrix}. \tag{3}$$

Note that the resonator is strongly detuned, as the diagonal element of the coupling matrix shows.

To implement this coupling matrix, it is necessary to examine carefully the field distributions of the resonating mode ($\mathrm{TM}_{110}$), as well as the $\mathrm{TE}_{10}$ mode, which is propagating, but nonresonating. For first fundamental investigations, a basic $\mathrm{TM}_{110}$ cavity is used that is directly coupled (without any iris) to the connecting waveguides (see insets in Fig. 3). Coupling of the $\mathrm{TM}_{110}$ resonance mode with the $\mathrm{TE}_{10}$ modes of the interface waveguides is obtained by employing proper centerline offsets between the waveguides and cavity. The $\mathrm{TM}_{110}$ mode would not be coupled in a centered structure and, therefore, small offsets correspond to weak couplings with the resonance mode. (Note that, in spite of the elementary structure used, the principal results also hold for configurations applying additionally inductive or capacitive irises at the interface ports.) To determine the sign of the bypass coupling at the input and output, we need to consider the phase of the propagating $\mathrm{TE}_{10}$ mode. If the magnetic field reverses direction at the output with respect to its direction at the input, a negative sign results in the coupling coefficient at the output with respect to the direct coupling coefficients. Since the bypass coupling is unique (represented by one coupling coefficient), such a sign reversal is best attributed to one of the direct couplings, either source to resonator or resonator to load. However, the coupling matrix in (3) requires no change in the relative signs of the coupling coefficients at the input and output. It is, therefore, necessary to introduce an additional sign change to compensate for the sign change due to the phase of $\mathrm{TE}_{10}$. This can be easily achieved when $\mathrm{TM}_{110}$ resonances are used to design the filter. Indeed, whereas the $\mathrm{TE}_{10}$ mode does not depend on the $y$-coordinate, the $H_x$-field component of the $\mathrm{TM}_{110}$ mode is an odd function of $y$ with respect to the center of the cross section of the waveguide. Here, $x$ and $y$ are the horizontal and vertical coordinates in the cross section of Fig. 3(a), for example. A relative sign change results when the coupling windows are located symmetrically with respect to a horizontal line through the center of the cross section of the waveguide.

With this arrangement, the overall relative signs of the coupling coefficients are all positive under the important assumption that the $\mathrm{TE}_{10}$ mode introduces a phase reversal between the input and output. (An implication of this assumption will be the presence of a spurious resonance in the lower stopband of the filter due to the $\mathrm{TE}_{10}$ resonance of the coupling windows,

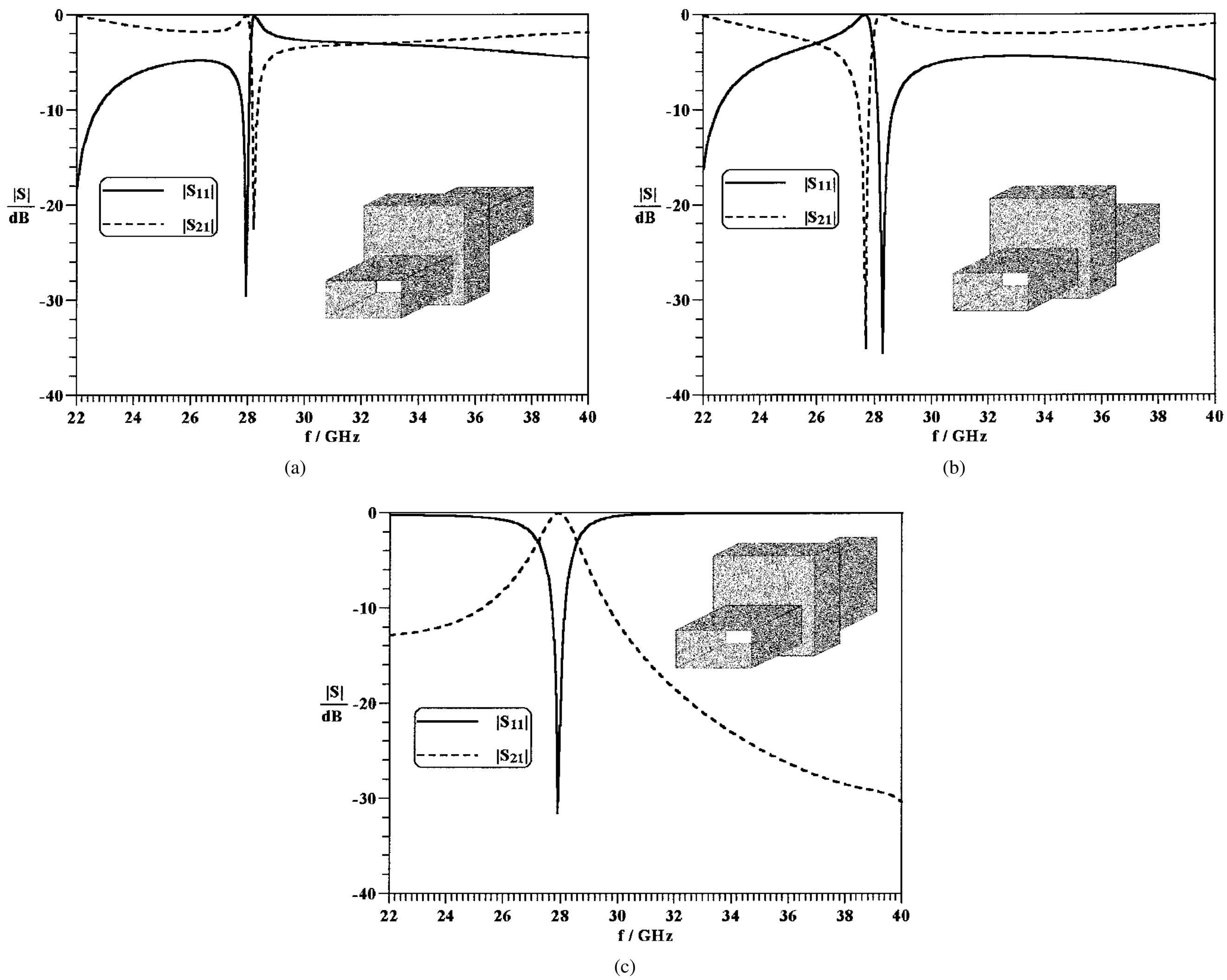


Fig. 3. Single $\mathrm{TM}_{110}$-mode cavity with: (a) transmission zero right, (b) left of the reflection zero, and (c) without transmission zero.

which is close to its cutoff frequency. Note that this spurious resonance is avoided when using additional inductive irises at the interface ports of the cavity.) The optimization of a structure based on the arrangement just described yields the response shown in Fig. 3(a). The presence of the transmission zero to the right-hand side of the reflection zero is evident. The transmission zero can be located arbitrarily close to the passband using this structure.

To insure flexibility in the design, it is necessary to be able to move the transmission zero in the previous structure to the lower side of the passband. An examination of the corresponding synthesis problem shows that the relative signs of the coupling coefficients at the input should be the opposite of those at the output. In other words, if the coupling coefficients are both positive at the input, one of them must be negative at the output. More specifically, if the transmission zero is located at $\Omega = -6$ and the in-band return loss is $R = 20$ dB, the following coupling matrix results:

$$M = \begin{bmatrix} 0.0000 & 1.3043 & 0.5647 \\ 1.3043 & 2.9877 & -1.3043 \\ 0.5647 & -1.3043 & 0.0000 \end{bmatrix}. \tag{4}$$

Again, under the assumption that the nonresonating $\mathrm{TE}_{10}$ mode introduces a relative sign change between the input and output, it is only necessary to place the coupling windows on the same side of a horizontal line through the center of the cross section. The resulting structure is symmetric, and a typical example is shown in Fig. 3(b) along with its response. The presence of the transmission zero in the lower stopband, i.e., below the reflection zero, is clearly observed.

From this discussion, it appears that transmission zeros will always be present since two paths for the signal are present at the source (and the load). Such an arrangement has been used to produce attenuation poles by other researchers [11]–[13]. For the structures used in this paper, there are two situations where the attenuation poles are eliminated, thereby producing a Chebychev response. The first one is the trivial case where input/output guides and irises are centered at the cavity interfaces. Of course, such a structure will not act as a $\mathrm{TM}_{110}$-mode filter since the $\mathrm{TM}_{11}$ mode will not be excited. The second case is shown in Fig. 3(c). Here, bypass couplings of the nonresonating $\mathrm{TE}_{10/01}$ cavity modes are suppressed by using interfaces with perpendicular orientation relative to each other [inset of Fig. 3(c)]. This arrangement is used in standard Chebyshev filters or whenever a certain bypass coupling needs to be eliminated (see Section III).

### B. Design of a Singlet

Although an exact and direct synthesis of the complete filters introduced here is not known at this time, it is possible to design, rather easily, individual singlets.

From the specifications of the filter, the coupling matrix of a singlet is first extracted using the technique introduced in [10]. The coupling matrix of such an arrangement is of the form [e.g., (3) and (4)]

$$M = \begin{bmatrix} 0 & x_1 & x_2 \\ x_1 & x_3 & \pm x_1 \\ x_2 & x_1 & 0 \end{bmatrix}. \tag{5}$$

The next step is to select the dimensions of the cross section of the cavity according to (1). The third dimension of the cavity is chosen to make sure that $\mathrm{TE}_{10}$ is nonresonating. To design the bypass coupling, we use the fact that the coupling from the input ($\mathrm{TE}_{10}$ in the feeding waveguide) to the nonresonating $\mathrm{TE}_{10}$ mode in the cavity is practically independent of the $y$-coordinate of the coupling aperture. We, therefore, place the input and output coupling apertures at the center of the cross section of the cavity. Under these conditions, $\mathrm{TM}_{110}$ is not excited in the cavity and the resulting scattering parameters from input to output are due to the bypass coupling alone. These scattering parameters can be easily determined using a field-theory-based analysis [14]. If these parameters are set equal to those of a two-port, which contains only the bypass coupling, it can be easily shown that $x_2$ in (5) satisfies the equation

$$x_2 = \frac{(1 - |S_{11}|)}{|S_{21}|}. \tag{6}$$

The size of the input and output apertures of the singlet are then adjusted until the value of $x_2$ obtained from (6) is identical to the one in the coupling matrix (5).

Following the principles outlined in Section II-A, we now move the input/output ports vertically away from their centered position. Depending on the vertical offset, the analysis will show a reflection zero and a transmission zero at normalized frequencies $\Omega_{zr}$ and $\Omega_{zt}$, respectively. The coupling coefficient $x_1$ is then given by

$$x_1 = \sqrt{\frac{\left|(\Omega_{zr} - \Omega_{zt})x_2\left(1 - x_2^2\right)\right|}{1 + x_2^2}}. \tag{7}$$

The positions of the input and output apertures are changed until $x_1$ given by (7) is identical to the value given by the coupling matrix in (5). To determine the frequency shift $x_3$, the dimensions of the cavity are changed until the center of the band is at the desired position. Note that, in this case, the center of the band differs from the location of the reflection zero.

As an example of the accuracy of the design, the values obtained from the synthesis [10] are compared to the final extracted values of the analysis. For the singlet shown in Fig. 3(b), the synthesized parameters of the coupling matrix are $x_1 = 1.5895$, $x_2 = 0.4588$, and $x_3 = 3.0536$. Through analysis, we obtain $x_1 = 1.6112$, $x_2 = 0.4375$, and $x_3 = 25.3597$. The large difference in $x_3$ is due to the loading of the cavity by the relatively large apertures. This loading is usually assumed to be negligible in the synthesis of the coupling matrix. Therefore, the parameter $x_3$ is determined by fine optimizing the singlet.

In the event of Fig. 3(c), where the bypass coupling is suppressed, $x_2 = 0$, and $x_1$ is extracted through

$$x_1 = \frac{1}{2}\sqrt{|\Delta\Omega_{3\ \mathrm{dB}}|}. \tag{8}$$

Here, $\Delta\Omega_{3\ dB} = \Omega_2 - \Omega_1$, where $\Omega_1$ and $\Omega_2$ are normalized frequencies at which $|S_{21}| = -3$ dB. The positions of the apertures are adjusted until the transmission performance shows the desired bandwidth. The cavity will then be detuned again to account for the loading.

### C. Two Cascaded Singlets

In order to provide additional design guidelines for the placement of transmission zeros, we proceed with inline arrangements of two $\mathrm{TM}_{110}$-mode cavities. These configurations are designed using overall optimization of two pre-synthesized singlets. Note that additional restrictions can now be imposed on the center iris. Following the previous explanations with respect to the inset of Fig. 3(a), it is obvious that a two-pole filter with two transmission zeros above the passband can be constructed by adding a second $\mathrm{TM}_{110}$-mode resonator, which reverses the offset of input/output waveguides shown in Fig. 3(a). The corresponding filter structure and its response are shown in Fig. 4(a) with transmission zeros at 29 and 29.6 GHz. Similarly, extending the structure in the inset of Fig. 3(b) by another cavity, but maintaining the vertical offsets of input/output guides and the coupling iris, will result in a two-pole filter with two transmission zeros below the passband. This is shown in Fig. 4(b) where the zeros are located at 25.45 and 25.75 GHz. Finally, the combination of a cavity arrangement of Fig. 3(a) with that of Fig. 3(b) will produce a two-pole filter with one transmission zero each above and below the passband. Fig. 4(c) shows the inline structure and its response. The zeros appear at 26.25 and 29.67 GHz.

Evidently, when more resonators are cascaded, more optimization is required, especially if some of the irises need to be changed to behave inductively (see Section III). Nevertheless, the pre-synthesized singlets clearly identify the transmission zeros and presence of a passband. Based on our experience, once the transmission zeros appear at their desired locations, the optimization process converges rapidly for this type of filters.

Spurious resonances and/or transmission zeros might appear well above or below the passband (cf. Fig. 4). They are usually caused by aperture resonances, as mentioned above, or by fundamental (e.g., $\mathrm{TE}_{101}$) or higher order mode resonances in the cavities. If required, they can be used as additional design parameters during the final optimization process. Alternatively, they can be shifted or their influence reduced by utilizing proper irises between cavities (see Section III).

## III. Results

Based on the design guidelines outlined above, a large variety of inline $\mathrm{TM}_{110}$-mode filters has been designed for operation in the lower $Ka$-band. Only a few examples will be presented here

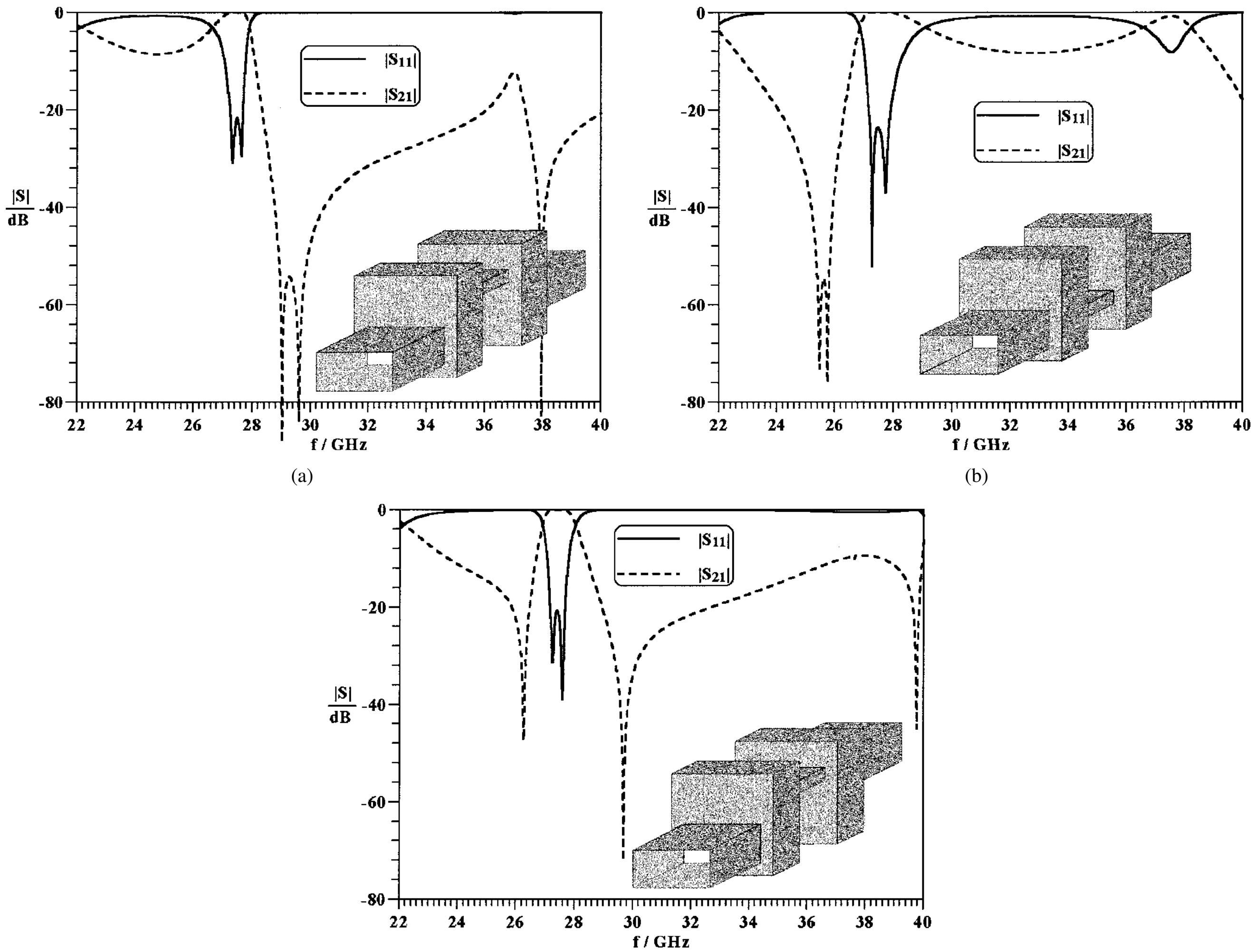


Fig. 4. Two-pole inline $\mathrm{TM}_{110}$-mode filters with: (a) two transmission zeros above the passband, (b) two transmission zeros below the passband, and (c) one transmission zero each above and below the passband.

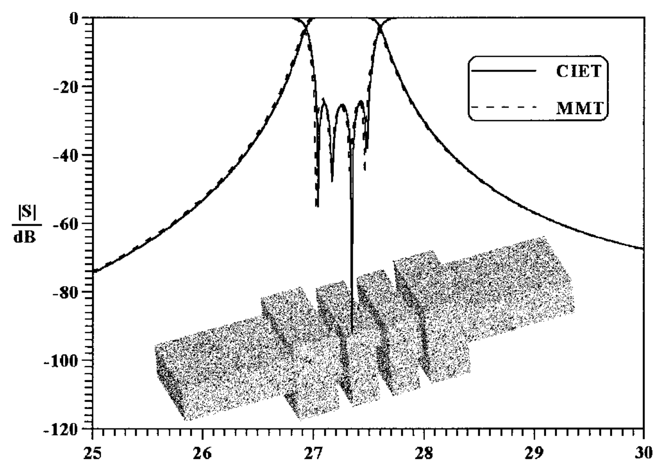


Fig. 5. Four-pole inline $\mathrm{TM}_{110}$-mode cavity filter with Chebyshev response.

to highlight the flexibility of the proposed filter and coupling structure.

Fig. 5 shows a four-pole $\mathrm{TM}_{110}$-mode filter satisfying a standard Chebyshev response by making use of the principle introduced in Fig. 3(c). Due to the arrangement of alternating 90° rotated interface ports and irises (couplings $M12$ and $M34$ exhibit perpendicular alignment; see inset of Fig. 5), $\mathrm{TE}_{10/01}$-mode bypass coupling is eliminated. Good agreement is observed between results of our coupled-integral-equation technique (CIET) [14] and an independently developed code based on the mode-matching technique (MMT).

The second design example produces an elliptic-function-type response shown in Fig. 6. The transmission zeros are realized separately using bypass couplings across the first and last resonator. In order to suppress any further bypass couplings, the iris between cavities 2 and 3 is vertically aligned (inset of Fig. 6). The different signs of the coupling sections required for the generation of the transmission zeros below and above the passband, respectively, are obtained by exploiting the principle explained above, i.e., one section provides iris offsets in the same direction, whereas the other one uses opposite offsets. The performance of the design is verified by comparison with the commercially available package $\mu$ WaveWizard.

Filter responses with more than two transmission zeros can be achieved by cascading singlets that produce the respective zeros in their individual responses. One such example is shown in Fig. 7. As seen in the inset of Fig. 7, cavities 1–3 are interfaced at the same side with respect to a horizontal line through

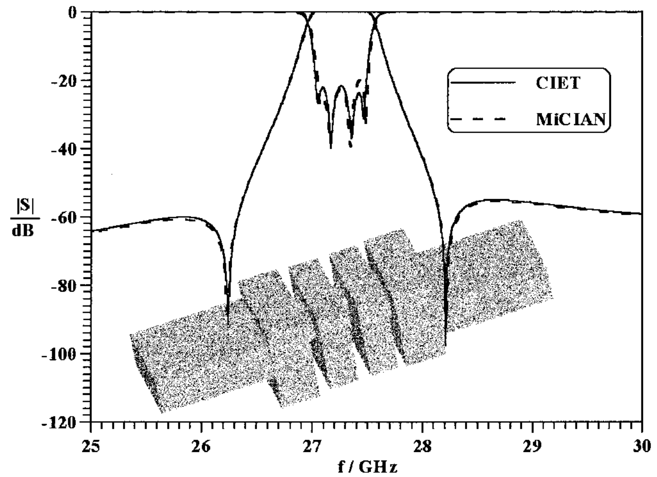


Fig. 6. Four-pole inline $\mathrm{TM}_{110}$-mode cavity filter with elliptic-function-type response and comparison with MiCIAN's $\mu$Wave Wizard.

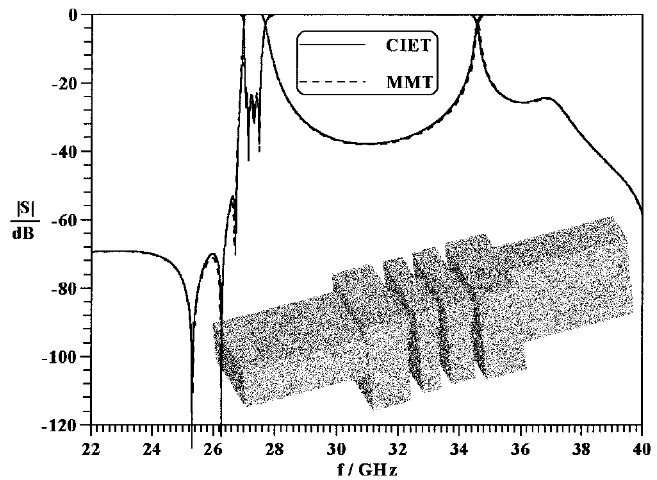


Fig. 7. Four-pole inline $\mathrm{TM}_{110}$-mode cavity filter with three transmission zeros below the passband.

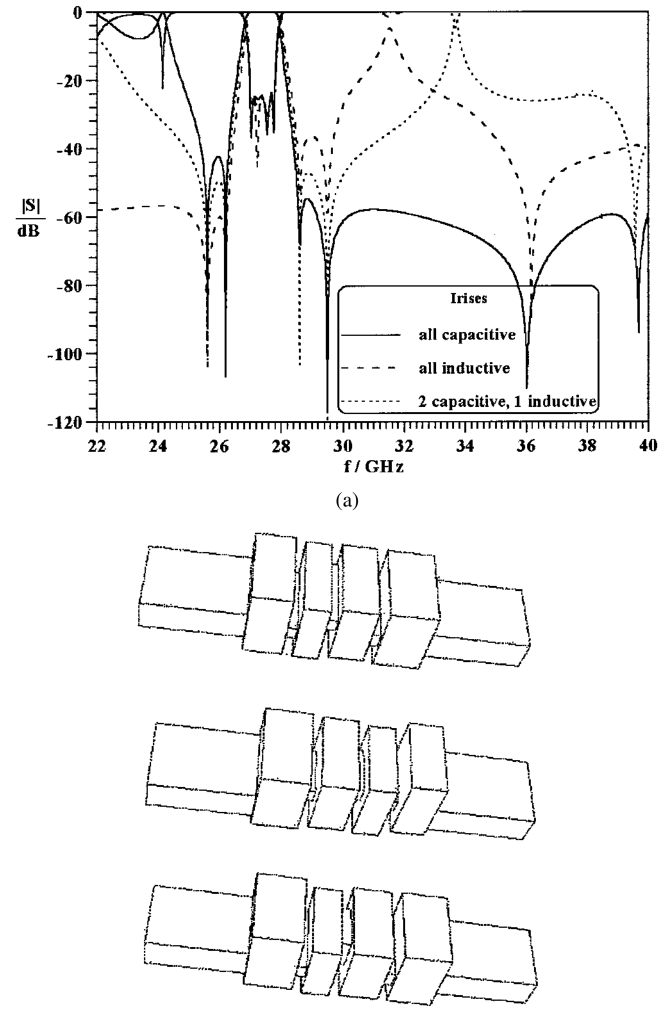


(a)

(b)

Fig. 8. (a) Responses of an inline four-pole $\mathrm{TM}_{110}$-mode filter with four transmission zeros. (b) Filter arrangements with only capacitive irises (top), only inductive irises (middle), two capacitive, and a center inductive iris (bottom).

the center of the cavity cross section. According to Fig. 3(b), this arrangement produces three transmission zeros below the passband, as shown in Fig. 7. The last possible transmission zero is suppressed by rotating the output waveguide by 90° with respect to the iris between cavity 3 and 4 [cf. Fig. 3(c)]. The possibility of rotating the output waveguide can be regarded as another degree of freedom, which adds to the design flexibility of the proposed filter structure. The parasitic passband at 34.55 GHz is due to a spurious $\mathrm{TE}_{10}$ resonance. The possibility of shifting such resonances is explained below.

This example is selected as the test case for realizability options. The four-pole filter in question has four transmission zeros, two below and two above the passband. Fig. 8(a) shows performances of three different possible realizations, which are sketched in Fig. 8(b). Whereas the three designs show the same passband characteristics and locations of transmission zeros, their behavior is distinctly different in frequency ranges away from the passband. The design with capacitive irises (solid lines in Fig. 8) shows the best attenuation performance toward higher frequencies. This basic property is well known from $E$-plane corrugated waveguide harmonic reject filters. However, due to the fact that all irises support at least $\mathrm{TE}_{10}$-mode propagation, there is only little rejection in the frequency range close to the cutoff frequency of the feeding waveguide (21 GHz). (This can be attributed to the $\mathrm{TE}_{10}$ resonance effect of the coupling windows (at the interface ports) and the capacitive irises; cf. [15]). A better selectivity in the lower stopband is achieved by inductive irises (dashed lines), which is well known from all-inductive iris filters, but their stopband performance at higher frequencies is compromised by iris resonances (here at 31.5 GHz). Of course, a combination of inductive and capacitive irises (dotted lines) will yield a performance that falls somewhere in between those of the two cases just discussed. Note that the transmission zeros at around 36 and 40 GHz are not included in the design process. They are due to the spurious $\mathrm{TE}_{101}$-mode resonances in the $\mathrm{TM}_{110}$-mode cavities and, if so desired, can be included in the final optimization of a filter.

In order to validate the entire $\mathrm{TM}_{110}$-mode filter design process, the configuration with all-capacitive irises was chosen for experimental verification. To facilitate an easier manufacturing process, the respective design in Fig. 8 has been modified to include milling radii. The fine optimization was carried out using MiCIAN's $\mu$Wave Wizard.

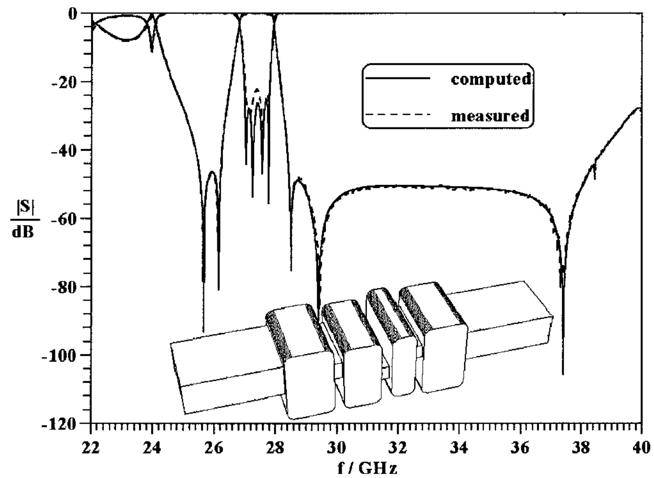


(a)

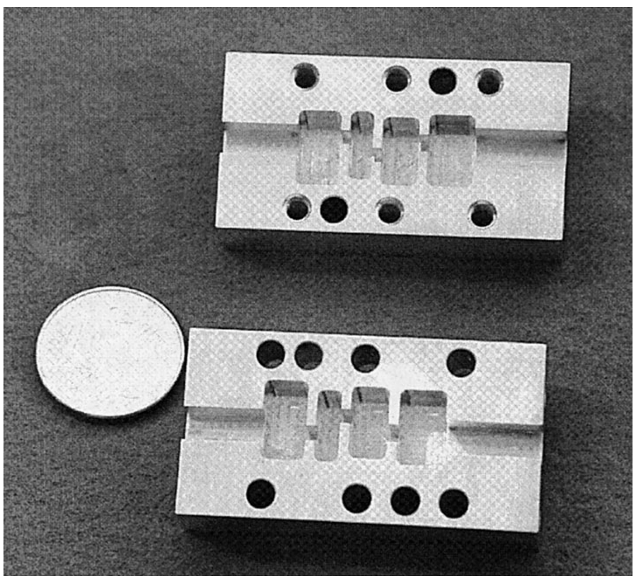

(b)

Fig. 9. (a) Comparison between computed and measured response of an inline four-pole $\mathrm{TM}_{110}$-mode filter with two transmission zeros below and two above the passband. (b) Photograph of the two halves of the $Ka$-band prototype and size comparison with a 1-Euro-cent coin.

Fig. 9(a) shows a direct comparison between the computed and measured data over a wide frequency range. Excellent agreement is observed. Only slight differences occur in the passband return loss at values below $-20$ dB. This is attributed to manufacturing tolerances of 0.02 mm. The measured insertion loss is less than 0.4 dB over a 700-MHz bandwidth. A photograph of the manufactured component is depicted in Fig. 9(b). Note that there are no post-assembly tuning devices added to the prototype filter. The excellent agreement between measured and computed data was obtained in the first prototype manufacturing process.

Finally, we would like to address the comparison of the $\mathrm{TM}_{110}$-mode configurations presented here with known types of pseudoelliptic rectangular waveguide filters. If we consider any other four-pole rectangular waveguide filter structure with four transmission zeros, we need at least four cross-couplings (including that of source to load) for the control of the four transmission zeros. However, each cross-coupling will affect the position of all transmission zeros. Consequently, the filter will require a large design and tuning effort to obtain a desired response with four transmission zeros. Moreover, the realization of the source–load coupling will most likely demand some sort of structural folding of the cavity arrangement.

Compared to such a scenario, the main advantages of our $\mathrm{TM}_{110}$-mode filters are, first, the structural simplicity of the inline configuration and, secondly, the individual control of each transmission zero.

## IV. Conclusions

Inline $\mathrm{TM}_{110}$-mode bandpass filters offer an attractive solution for the design of pseudoelliptic rectangular waveguide filters. These filters have simple geometries, which lend themselves to design by accurate and fast computer-aided design (CAD) tools, but retain a high flexibility as to the number and locations of transmission zeros. Wide stopbands can be achieved by carefully selecting the coupling irises. A variety of design examples have been presented; and excellent agreement with measured data has been demonstrated.

## References

[1] A. Atia and A. E. Williams, "New type of waveguide bandpass filters for satellite transponders," *COMSAT Tech. Rev.*, vol. 1, no. 1, pp. 21–43, 1971.

[2] A. E. Williams, "A four-cavity elliptic waveguide filter," *IEEE Trans. Microwave Theory Tech.*, vol. MTT-18, pp. 1109–1114, Dec. 1970.

[3] R. J. Cameron, "General prototype network synthesis methods for microwave filters," *ESA J.*, vol. 6, pp. 193–206, 1982.

[4] ——, "General coupling matrix synthesis methods for Chebyshev filtering functions," *IEEE Trans. Microwave Theory Tech.*, vol. 47, pp. 433–442, Apr. 1999.

[5] J. D. Rhodes and R. J. Cameron, "General extracted pole synthesis technique with application to low-loss $\mathrm{TE}_{011}$-mode filters," *IEEE Trans. Microwave Theory Tech.*, vol. MTT-28, pp. 1018–1028, Sept. 1980.

[6] S. Amari and J. Bornemann, "Using frequency-dependent coupling to generate finite attenuation poles in direct-coupled resonator bandpass filters," *IEEE Microwave Guided Wave Lett.*, vol. 9, pp. 404–406, Oct. 1999.

[7] F. Arndt, T. Duschak, U. Papziner, and P. Rolappe, "Asymmetric iris coupled filters with stopband poles," in *IEEE MTT-S Int. Microwave Symp. Dig.*, Dallas, TX, May 1990, pp. 215–218.

[8] M. Guglielmi, F. Montauti, and P. Arcioni, "Implementing transmission zeros in inductive-window bandpass filter," *IEEE Trans. Microwave Theory Tech*, vol. 43, pp. 1911–1915, Aug. 1995.

[9] U. Rosenberg and W. Hägele, "Consideration of parasitic bypass couplings in overmoded cavity filter designs," *IEEE Trans. Microwave Theory Tech.*, vol. 42, pp. 1301–1306, July 1994.

[10] S. Amari, U. Rosenberg, and J. Bornemann, "Adaptive synthesis and design of resonator filters with source/load-multi-resonator coupling," *IEEE Trans. Microwave Theory Tech.*, vol. 50, pp. 1969–1978, Aug. 2002.

[11] I. Hunter, D. Rhodes, and V. Dassonville, "Dual-mode filters with conductor-loaded dielectric resonators," *IEEE Trans. Microwave Theory Tech.*, vol. 47, pp. 2304–2311, Dec. 1999.

[12] J. Liang and W. Blair, "High-$Q$ TE01 mode DR filters for PCS wireless base stations," *IEEE Trans. Microwave Theory Tech.*, vol. 46, pp. 2493–2500, Dec. 1998.

[13] L. Accatino, G. Bertin, M. Mongiardo, and G. Resnati, "A new dielectric-loaded dual-mode cavity for mobile communications filters," in *31st Eur. Microwave Conf.*, vol. 1, Sept. 2001, pp. 37–40.

[14] J. Bornemann, U. Rosenberg, S. Amari, and R. Vahldieck, "Edge-conditioned vector basis functions for the analysis and optimization of rectangular waveguide dual-mode filters," in *IEEE MTT-S Int. Microwave Symp. Dig.*, Anaheim, CA, June 1999, pp. 1695–1698.

[15] J. Uher, J. Bornemann, and U. Rosenberg, *Waveguide Components for Antenna Feed Systems: Theory and CAD*. Boston, MA: Artech House, 1999, pp. 230–231.

**Uwe Rosenberg** (M'90–SM'93) received the Dipl. Ing. degree (first-class honors) in electrical engineering (telecommunication technique) from the Fachhochschule der Deutschen Bundespost, Dieburg, Germany, in 1982.

From 1982 to 1983, he was with Hydro Therm, Dieburg, Germany, where he was involved with the design and development of automatic safety and heating control circuits. From 1983 to 1985, he was with the Technische Hochschule Darmstadt, Darmstadt, Germany, where he was involved with the design and development of experimental installations and software components for microcomputer control systems. In 1985, he joined the Space Division, ANT Nachrichtentechnik GmbH (now Tesat-Spacecom GmbH & Company KG), Backnang, Germany, where he was engaged in research and development on microwave filters, multiplexers, and passive subsystems for communications satellites. Since 1989, he has been Head of the Research and Development Laboratory for Passive Microwave Components and Subsystems, Marconi Communications GmbH (formerly Bosch Telecom GmbH, Public Networks Division), Backnang, Germany, where he has been responsible for research and development of integrated waveguide transceiver circuitries, channel branching networks (multiplexers), antenna feed and waveguide (feeder) systems for trunk and access radio applications, mobile base-stations, large Earth stations, and communications satellites. He coauthored *Waveguide Components for Antenna Feed Systems: Theory and CAD* (Norwood, MA: Artech House, 1993). He has also authored or coauthored over 50 technical papers. He holds 36 microwave design patents

Mr. Rosenberg is a member of Verband der Elektrotechnik Elektronik Informationstechnik (VDE), Informationstechnische Gesellschaft (ITG), and Verein Deutscher Ingenieure (VDI). He is a senior member of the IEEE Microwave Theory and Techniques Society (IEEE MTT-S) and the IEEE Antennas and Propagation Society (IEEE AP-S).

**Smain Amari** (M'98) received the DES degree in physics and electronics from Constantine University, Constantine, Algeria, in 1985, and the Master's degree in electrical engineering and Ph.D. degree in physics from Washington University, St. Louis, MO, in 1989 and 1994, respectively.

From 1994 to 2000, he was with the Department of Electrical and Computer Engineering, University of Victoria, Victoria, BC, Canada. From 1997 to 1999, he was a Visiting Scientist with the Swiss Federal Institute of Technology, Zurich, Switzerland, and a Visiting Professor in Summer 2001. Since November 2000, he has been with the Department of Electrical and Computer Engineering, Royal Military College of Canada, Kingston, ON, Canada, where he is currently an Associate Professor. He is interested in numerical analysis, numerical techniques in electromagnetics, applied physics, applied mathematics, wireless and optical communications, CAD of microwave components, applied physics, and application of quantum field theory in quantum many-particle systems.

**Jens Bornemann** (M'87–SM'90–F'02) received the Dipl.-Ing. and Dr.-Ing. degrees in electrical engineering from the University of Bremen, Bremen, Germany, in 1980 and 1984, respectively.

From 1984 to 1985, he was a Consulting Engineer. In 1985, he joined the University of Bremen, as an Assistant Professor. Since April 1988, he has been with the Department of Electrical and Computer Engineering, University of Victoria, Victoria, BC, Canada, where he became a Professor in 1992. From 1992 to 1995, he was a Fellow of the British Columbia Advanced Systems Institute. In 1996, he was a Visiting Scientist with Spar Aerospace Limited (now EMS Technologies Inc.), Ste-Anne-de-Bellevue, QC, Canada, and a Visiting Professor with the Microwave Department, University of Ulm, Ulm, Germany. From 1997 to 2002, he was a Co-Director of the Center for Advanced Materials and Related Technology (CAMTEC), University of Victoria. He coauthored *Waveguide Components for Antenna Feed Systems. Theory and Design* (Norwood, MA: Artech House, 1993) and has authored/coauthored over 180 technical papers. His research activities include RF/wireless/microwave/millimeter-wave components and systems design, and problems involving electromagnetic-field theory in integrated circuits, feed networks, and radiating structures.

Dr. Bornemann is a Registered Professional Engineer in the Province of British Columbia, Canada. He serves on the Technical Program Committee of the IEEE Microwave Theory and Techniques Society (IEEE MTT-S) International Microwave Symposium (IMS) and the Editorial Advisory Board of the *International Journal of Numerical Modeling*. From 1999 to 2002, he was an associate editor of the IEEE TRANSACTIONS ON MICROWAVE THEORY AND TECHNIQUES in the area of microwave modeling and CAD.